

Realising Synthetic Active Inference Agents, Part II: Variational Message Updates

Thijs van de Laar¹, Magnus Koudahl^{1,2}, and Bert de Vries^{1,3}

¹Department of Electrical Engineering, Eindhoven University of
Technology, Eindhoven, The Netherlands

²VERSES Research Lab, Eindhoven, The Netherlands

³GN Hearing Benelux BV, Eindhoven, The Netherlands

June 6, 2023

Abstract

The Free Energy Principle (FEP) describes (biological) agents as minimising a variational Free Energy (FE) with respect to a generative model of their environment. Active Inference (AIF) is a corollary of the FEP that describes how agents explore and exploit their environment by minimising an expected FE objective. In two related papers, we describe a scalable, epistemic approach to synthetic AIF agents, by message passing on free-form Forney-style Factor Graphs (FFGs). A companion paper (part I) introduces a Constrained FFG (CFFG) notation that visually represents (generalised) FE objectives for AIF. The current paper (part II) derives message passing algorithms that minimise (generalised) FE objectives on a CFFG by variational calculus. A comparison between simulated Bethe and generalised FE agents illustrates how synthetic AIF induces epistemic behaviour on a T-maze navigation task. With a full message passing account of synthetic AIF agents, it becomes possible to derive and reuse message updates across models and move closer to industrial applications of synthetic AIF.

Keywords: Free Energy Principle, Active Inference, Variational Optimisation, Variational Message Passing

1 Introduction

The Free Energy Principle (FEP) postulates that the behaviour of biological agents can be modelled as minimising a Variational Free Energy (VFE) [9]. Active Inference (AIF) is a corollary of the FEP that describes how agents propose effective actions by minimising an Expected Free Energy (EFE) objective that internalises a Generative Model (GM) of the agent’s environment and a prior belief about desired outcomes [11, 10].

Traditional approaches describe AIF in terms of variational inference in the context of a partially observable Markov decision process [5]. Simulated agents then engage in information-seeking behaviour and automatically trade off exploratory and exploitative modes [10]. However, these methods do not readily scale to free-form models.

Variational objectives for AIF can be minimised by message passing on a Forney-style Factor Graph (FFG) representation of the GM. Several authors have attempted to scale AIF under this message passing framework [29, 7]. However, agents based on these approaches lack crucial epistemic characteristics [25, 30].

In two related papers, we describe a message passing approach to scalable, synthetic AIF agents. In part I, we identify a hiatus in the AIF problem specification language [15]. Specifically, we recognise that optimisation constraints [27] are not included in the present-day FFG notation, which may lead to ambiguous problem descriptions. Part I introduces a Constrained FFG (CFFG) notation for constraint specification on FFGs, and illustrate how free energy objectives, including the Generalised Free Energy (GFE) [21], relate to specific constraints and message passing schedules.

In part II, which is the current paper, we use the CFFG notation as introduced in part I to define locally constrained variational objectives, and derive variational message updates for GFE-based control using variational calculus. The resulting control algorithms then induce epistemic behaviour in synthetic AIF agents. We reason purely from an engineering point-of-view and do not concern ourselves with biological plausibility.

In this paper, our contributions are three-fold:

- We use variational calculus to derive general message update expressions for GFE-based control in synthetic AIF agents;
- We derive specialised messages for a discrete-variable model that is often used for AIF control in practice;
- We implement these results in a reactive programming framework and simulate a perception-action cycle on the T-maze navigation task.

With a full message passing account and reactive implementation of GFE optimisation, it becomes possible to derive and reuse custom message updates across models and get a step closer to realising scalable synthetic AIF agents for industrial applications.

In Sec. 2 we review variational Bayes as a constrained optimisation problem that can be solved by message passing on a Constrained FFG (CFFG). In Sec. 3

we review AIF and formulate perception, learning and control as message passing on a CFFG. In Sec. 4, we focus on the constraint definition around a submodel of two facing nodes and derive stationary solutions and messages for GFE-based control. In Sec. 5 we apply these general results to a specific discrete-variable goal-observation submodel that is often used in AIF practice. We then work towards implementation in a simulated setting and describe a perception-action cycle in terms of time-dependent constraints in Sec. 6. The T-maze task is described in Sec. 7 and simulated in a reactive programming framework in Sec. 8. We finish with a summary of related work in Sec. 9, and our conclusions in Sec. 10.

2 Review of Variational Message Passing

In this section we briefly review Variational Message Passing (VMP) as a distributed approach to minimising Variational Free Energy (VFE) objectives. We start by reviewing variational Bayes and then review a visual representation of constrained VFE objectives on a Constrained Forney-style Factor Graph (CFFG).

2.1 Variational Bayes

Given a probabilistic model and some observed data, Bayesian inference concerns the computation of posterior distributions over variables of interest. Because Bayesian inference is intractable in general, the Bayesian inference problem is often converted to a constrained variational optimisation problem. The optimisation objective for the so-called variational Bayes approach is an information-theoretic quantity known as the Variational Free Energy (VFE),

$$F[q] = \mathbb{E}_q \left[\log \frac{q(\mathbf{s})}{f(\mathbf{s})} \right],$$

comprised of a probabilistic model f over some generic variables \mathbf{s} and a variational distribution q . As a notational convention, we write a collection of variables in cursive bold script. An overview of notational conventions is available in Table 1. The VFE is optimised under a set of constraints \mathcal{Q} , as

$$q^* = \arg \min_{q \in \mathcal{Q}} F[q].$$

The VFE conveniently imposes an upper bound on the Bayesian surprise (i.e., the negative logarithm of model evidence Z). Minimisation then renders the VFE a close approximation to the surprise, while the variational distribution becomes a close approximation to the (intractable) exact posterior p . Then at the minimum,

$$F[q^*] = \underbrace{-\log Z}_{\text{surprise}} + \underbrace{\text{KL}[q^* \| p]}_{\text{posterior divergence}},$$

with KL the Kullback-Leibler divergence.

Symbol	Explanation
s_i	Generic variable with index i
\mathbf{s}	Collection of variables
$\mathbf{s}_{\setminus j}$	Collection excluding s_j
$\underline{\mathbf{s}}$	Sequence of past variables
$\overline{\mathbf{s}}$	Sequence of future variables
\mathbf{s}	Vector
\mathbf{S}	Matrix
$\bar{\mathbf{s}}$	Expectation of a vector variable
z, w	State variables
x	Observation variable
θ, ϕ	Parameters
f	Factor function (possibly unnormalised)
p	Probability distribution
q	Variational distribution
\mathcal{Q}	Constraint set
\mathcal{G}	Forney-style factor (sub)graph
\mathcal{V}	Nodes
\mathcal{E}	Edges
F	Variational free energy
G	Generalised free energy
H	Entropy
U	Average energy
L	Lagrangian
λ, ψ	Lagrange multipliers
μ	Message

Table 1: Overview of notational conventions.

Acronym	Explanation
FEP	Free Energy Principle
VFE	Variational Free Energy
AIF	Active Inference
EFE	Expected Free Energy
GM	Generative Model
FFG	Forney-style Factor Graph
GFE	Generalised Free Energy
CFFG	Constrained FFG
VMP	Variational Message Passing
BFE	Bethe Free Energy
SSM	State-Space Model

Table 2: Overview of acronyms.

2.2 Forney-Style Factor Graphs

A Forney-style Factor Graph (FFG) $\mathcal{G} = (\mathcal{V}, \mathcal{E})$ can be used to graphically represent a factorised function, with nodes \mathcal{V} and edges \mathcal{E} . Given a factorised model,

$$f(\mathbf{s}) = \prod_{a \in \mathcal{V}} f_a(\mathbf{s}_a),$$

edges in the corresponding FFG represent variables and nodes represent (probabilistic) relationships between variables [8]. As an example, consider the model

$$f(\mathbf{s}) = f_a(s_1, s_3) f_b(s_1, s_2, s_4) f_c(s_2, s_5) f_d(s_5),$$

for which the FFG is depicted in Fig. 1 (top left).

Note that edges in an FFG connect to at most two nodes. Therefore, equality factors are used to effectively duplicate variables for use in more than two factors. Technically, the equality factor $f_{=}(s_i, s_j, s_k) = \delta(s_i - s_j) \delta(s_i - s_k)$ constrains variables on connected edges to be equal through (Dirac or Kronecker) delta functions.

2.3 Bethe Lagrangian Optimisation

We can now use the factorisation of the model to induce a Bethe factorisation on the variational distribution

$$q(\mathbf{s}) \triangleq \prod_{a \in \mathcal{V}} q_a(\mathbf{s}_a) \prod_{i \in \mathcal{E}} q_i(s_i)^{1-d_i},$$

with d_i the degree of edge i .

Substituting the Bethe factorisation in the VFE, the resulting Bethe Free Energy (BFE) then factorises into node- and edge-local contributions. As is common in probabilistic notation, we assume that factors in the model and variational distribution are indexed by their argument variables (where context allows). The BFE then factorises into node- and edge-local contributions, as

$$F[q] \triangleq \sum_{a \in \mathcal{V}} \overbrace{\mathbb{E}_{q(\mathbf{s}_a)} \left[\log \frac{q(\mathbf{s}_a)}{f(\mathbf{s}_a)} \right]}^{\text{local free energy } F[q_a]} - \sum_{i \in \mathcal{E}} \overbrace{-\mathbb{E}_{q(s_i)} [\log q(s_i)] (1 - d_i)}^{\text{local entropy } H[q_i]}.$$

Using Lagrange multipliers, we can convert the optimisation problem on \mathcal{Q} to a free-form optimisation problem of a Lagrangian, where Lagrange multipliers enforce local (e.g. normalisation and marginalisation) constraints. The fully

localised optimisation objective then becomes

$$\begin{aligned}
L[q] \triangleq & \sum_{a \in \mathcal{V}} F[q_a] - \sum_{i \in \mathcal{E}} (1 - d_i) H[q_i] + \\
& \sum_{a \in \mathcal{V}} \psi_a \left(\int q(\mathbf{s}_a) d\mathbf{s}_a - 1 \right) + \sum_{i \in \mathcal{E}} \psi_i \left(\int q(s_i) ds_i - 1 \right) + \\
& \sum_{a \in \mathcal{V}} \sum_{i \in \mathcal{E}(a)} \int \lambda_{ia}(s_i) \left(q(s_i) - \int q(\mathbf{s}_a) d\mathbf{s}_{a \setminus i} \right) ds_i,
\end{aligned}$$

which is optimised for

$$q^*(\mathbf{s}) = \arg \min_q L[q],$$

over the individual terms in the variational distribution factorisation.

The belief propagation algorithm [23] has been formulated in terms of Bethe Lagrangian optimisation by message passing on factor graphs [33]. Additional factorisation of the variational distribution induces structured and mean-field Variational Message Passing (VMP) algorithms [6]. A comprehensive overview of constraint manipulation and resulting message passing algorithms is available in [27].

2.4 Constrained Forney-Style Factor Graphs

An FFG alone does not unambiguously define a constrained VFE objective, and a full expression for a localised Lagrangian alongside an FFG can become quite verbose. A visual representation may help interpret and disambiguate variational objectives and constraints. The resulting Constrained FFG (CFFG) notation is introduced in detail by our companion paper [15].

In brief, a CFFG is constructed from an FFG according to the following rules:

- Beads represent normalised variational distributions;
- Beads on nodes and edges represent node- and edge-local terms in the factorised variational distribution respectively;
- A connection between beads indicates a marginalisation constraint;
- Multiple beads within a node represent a factorisation constraint;
- A solid bead with inscribed delta indicates a data constraint;
- A square bead indicates a p-substitution (Sec. 3.3.2).

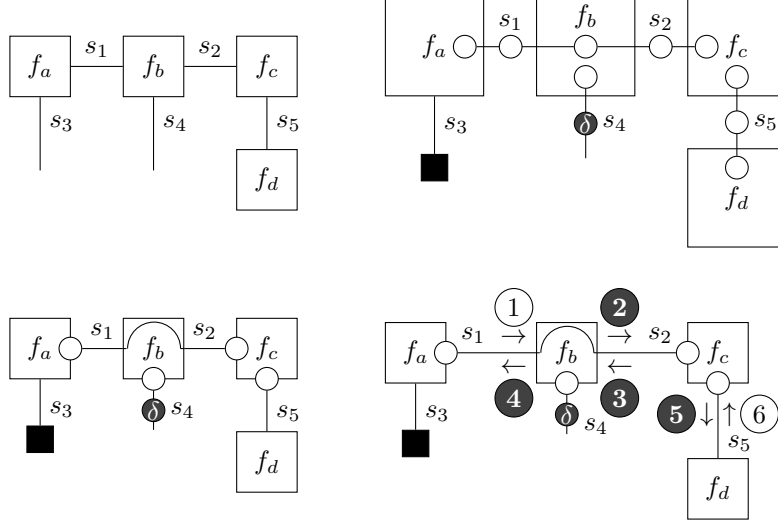


Figure 1: Example Forney-style factor graph (top left), with an explicit (top right) and corresponding compressed (bottom left) CFFG, and resulting messages (bottom right). The solid square indicates a clamped variable, and the solid circle a data constraint. Sum-product and variational messages are indicated by white and dark message circles respectively.

2.4.1 Explicit Notation

As an example, consider the CFFG of Fig. 1 (top right), which corresponds to a VFE objective of the form

$$F[q] = \mathbb{E}_{q(\mathbf{s}_{\setminus 3})} \left[\log \frac{q(\mathbf{s}_{\setminus 3})}{f(\mathbf{s}_{\setminus 3} | s_3 = \hat{s}_3)} \right].$$

Bead chains indicate normalised local variational distributions under a Bethe factorisation, connected by local marginalisation. The delta-inscribed bead indicates a data-constraint, which is enforced by a specific marginalisation constraint of the form

$$\iint q_b(s_1, s_2, s_4) ds_1 ds_2 \triangleq \delta(s_4 - \hat{s}_4).$$

Note that we define two ways to indicate given values. Namely, a solid square represents an a-priori given (clamped) value, and a solid delta bead represents a data constraint on the variational distribution [3, 27]. This notation thus differs from the standard notation, where all clamped values (including data) are represented by a black squares [24].

The example CFFG also imposes factorisation constraints,

$$\begin{aligned} q_b(s_1, s_2, s_4) &\triangleq q_b(s_1, s_2)q_b(s_4) \\ q_c(s_2, s_5) &\triangleq q_c(s_2)q_c(s_5), \end{aligned}$$

as represented by multiple beads inside the corresponding nodes.

2.4.2 Compressed Notation

The explicit CFFG in Fig. 1 (top right) is comprehensive but also visually a bit verbose. Therefore, we summarise in Fig. 1 (bottom left) a compressed CFFG notation as introduced by our companion paper [15].

In the compressed CFFG, bead chains are represented only by their terminating beads. For brevity, connections that internally cross a node are not drawn if all beads on the adjacent edges are connected. This way, the compressed CFFG only emphasises constraints (e.g., structured factorisations and data constraints) that deviate from the “standard” Bethe constraints. We will use the explicit and compressed CFFG notation in the context of full- and sub-models respectively.

2.4.3 Variational Message Passing

The resulting message passing schedule for the CFFG example is indicated in Fig. 1 (bottom right). White circles indicate messages that are computed by sum-product updates [18] and dark circles indicate variational message updates [6].

3 Review of Active Inference by Variational Message Passing

In this section we work towards a message passing formulation of synthetic AIF. We start by reviewing AIF and the CFFG representation for a GFE objective for control. Further details on variational objectives for AIF and epistemic considerations can be found in [15].

3.1 Active Inference

AIF defines an agent and an environment that are separated by a Markov blanket [13]. In general, at each time step, the agent sends an action to the environment. In turn, the environment responds with an outcome that is observed by the agent. The goal of the agent is to manipulate the environment to elicit desired outcomes.

A Generative Model (GM) defines a joint probability distribution that represents the agent’s beliefs about how interventions in the environment lead to observable outcomes. In order to propose effective interventions, the agent must perform the tasks of perception, learning and control. AIF performs these tasks by (approximate) Bayesian inference on the GM, by inferring states, parameters and controls, respectively.

3.2 Generative Model Definition

We assume that an agent operates in a dynamical environment, and define a sequence of state variables $\mathbf{z} = (z_0, z_1, \dots, z_N)$ that model the time-dependent latent state of the environment. We also assume that the agent may influence the environment, as modelled by controls $\mathbf{u} = (u_1, \dots, u_N)$, which indirectly affect observations $\mathbf{x} = (x_1, \dots, x_N)$. Finally, we define model parameters $\boldsymbol{\theta}$. We assume that parameters evolve at a slower temporal scale than the states, and can therefore be effectively considered time-independent.

The GM then defines a joint distribution $p(\mathbf{x}, \mathbf{z}, \boldsymbol{\theta}, \mathbf{u})$ that represents the agent’s belief about how controls affect states and observations under some parameters. A first-order Markov assumption then imposes a conditional independence between states [14]. The GM then factorises as a State-Space Model (SSM),

$$p(x, z, \theta, u) = \underbrace{p(z_0)}_{\text{state prior}} \underbrace{p(\theta)}_{\text{parameter prior}} \prod_{k=1}^T \underbrace{p(x_k | z_k, \theta)}_{\text{observation model}} \underbrace{p(z_k | z_{k-1}, u_k)}_{\text{transition model}} \underbrace{p(u_k)}_{\text{control prior}}, \quad (1)$$

where we assumed a parameterised observation model. The SSM of (1) can be graphically represented by the FFG of Fig. 2.

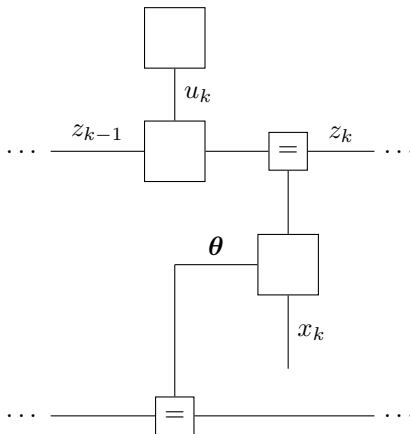


Figure 2: A single slice of the Forney-style factor graph representation of the generative model of (1). State and parameter priors not drawn.

3.3 Message Passing

In this section we formulate synthetic AIF as a message passing procedure on a model of past and future states. Inference on a model of past states then relates to perception and learning, while inference on a model of future states relates to control.

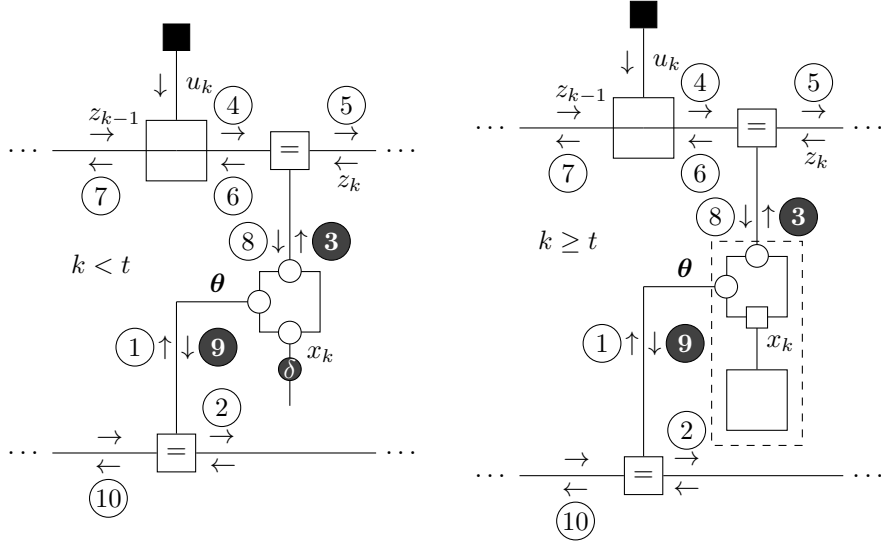


Figure 3: Constrained Forney-style factor graph representations for variational objectives on models for past (left) and future states (right). The dashed box indicates a composite structure for the goal-observation submodel.

3.3.1 Model of Past States

With t the present time, we denote sequences of past variables $\underline{x} = \mathbf{x}_{<t}$, $\underline{z} = \mathbf{z}_{<t}$ (including z_0), and $\underline{u} = \mathbf{u}_{<t}$. A model of past states can then be constructed from (1), as

$$p(\underline{x}, \underline{z}, \theta | \underline{u}) = p(\theta) p(z_0) \prod_{k=1}^{t-1} p(x_k | z_k, \theta) p(z_k | z_{k-1}, u_k).$$

Instead of presenting the VFE objective and constraints in formulas, we draw the CFFG for past states in Fig. 3 (left). The indicated message passing schedule defines a forward and backward pass on the CFFG. The forward pass, comprised of messages ① – ⑤, represents inference for perception where (hierarchical) states are estimated by a filtering procedure. The combined forward-backward pass represents inference for learning, where all past information is incorporated to infer a posterior over parameters by a smoothing procedure. These posteriors can then be used as (empirical) priors in the model of future states.

3.3.2 Model of Future States

AIF for control infers a posterior belief over policies from a free energy objective that is defined with respect to a model of future states. We define sequences of future (including present) variables $\bar{x} = \mathbf{x}_{\geq t}$, $\bar{z} = \mathbf{z}_{\geq t-1}$ (including z_{t-1}), and $\bar{u} = \mathbf{u}_{\geq t}$. Because future outcomes are by definition unobserved, we include goal

priors on the future observation variables. From the GM of (1), we construct the model of future states, as

$$f(\bar{\mathbf{x}}, \bar{\mathbf{z}}, \boldsymbol{\theta}, \bar{\mathbf{u}}) = p(z_{t-1})p(\boldsymbol{\theta}) \prod_{k=t}^T p(x_k|z_k, \boldsymbol{\theta})p(z_k|z_{k-1}, u_k)p(u_k) \underbrace{\tilde{p}(x_k)}_{\text{goal prior}},$$

with T a lookahead time horizon. The (empirical) state and parameter prior follow from message passing for perception and learning, respectively. Note that the model of future states is unnormalised as a result of simultaneous constraints on $\bar{\mathbf{x}}$ by the observation models and the goal priors.

We then define a VFE objective for control, as

$$\begin{aligned} F[q] &\triangleq \mathbb{E}_{q(\bar{\mathbf{x}}, \bar{\mathbf{z}}, \boldsymbol{\theta}, \bar{\mathbf{u}})} \left[\log \frac{q(\bar{\mathbf{x}}, \bar{\mathbf{z}}, \boldsymbol{\theta}, \bar{\mathbf{u}})}{f(\bar{\mathbf{x}}, \bar{\mathbf{z}}, \boldsymbol{\theta}, \bar{\mathbf{u}})} \right] \\ &= \mathbb{E}_{q(\bar{\mathbf{u}})} \left[\log \frac{q(\bar{\mathbf{u}})}{p(\bar{\mathbf{u}})} + \underbrace{\mathbb{E}_{q(\bar{\mathbf{x}}, \bar{\mathbf{z}}, \boldsymbol{\theta}|\bar{\mathbf{u}})} \left[\log \frac{q(\bar{\mathbf{x}}, \bar{\mathbf{z}}, \boldsymbol{\theta}|\bar{\mathbf{u}})}{f(\bar{\mathbf{x}}, \bar{\mathbf{z}}, \boldsymbol{\theta}|\bar{\mathbf{u}})} \right]}_{F[q; \bar{\mathbf{u}}]} \right], \end{aligned}$$

which (under normalisation) is minimised by

$$q^*(\bar{\mathbf{u}}) = \sigma(-F(\bar{\mathbf{u}})),$$

with σ a softmax function and

$$F(\bar{\mathbf{u}}) = \min_{q \in \mathcal{Q}} F[q; \bar{\mathbf{u}}],$$

the optimal VFE value conditioned on the policy $\bar{\mathbf{u}}$. This solution thus constructs a posterior over a selection of policies by evaluating their respective free energies. In the current paper we simply select the policy with the lowest free energy.

The conditioning of the variational distribution on $\bar{\mathbf{u}}$ is implied by the conditioning of the GM on $\bar{\mathbf{u}}$. Technically, the variational distribution is always conditioned on the values on which the underlying model is conditioned. Therefore we omit this explicit conditioning in the variational density.

We now impose a factorisation constraint

$$q(\bar{\mathbf{x}}, \bar{\mathbf{z}}, \boldsymbol{\theta}) \triangleq q(\bar{\mathbf{z}})q(\boldsymbol{\theta}) \prod_{k=t}^T q(x_k),$$

and substitute *only the expectation terms* with their respective observation models

$$q(x_k) \rightarrow p(x_k|z_k, \boldsymbol{\theta}) \text{ in exp. terms for all } k \geq t. \quad (2)$$

This so-called p-substitution is introduced by our companion paper [15], and transforms the VFE to a Generalised Free Energy (GFE) objective [21],

$$G[q; \bar{\mathbf{u}}] = \mathbb{E}_{p(\bar{\mathbf{x}}|\bar{\mathbf{z}}, \boldsymbol{\theta})q(\bar{\mathbf{z}})q(\boldsymbol{\theta})} \left[\log \frac{q(\bar{\mathbf{x}})q(\bar{\mathbf{z}})q(\boldsymbol{\theta})}{f(\bar{\mathbf{x}}, \bar{\mathbf{z}}, \boldsymbol{\theta}|\bar{\mathbf{u}})} \right]. \quad (3)$$

For convenience, we write $p(\bar{\mathbf{x}}|\bar{\mathbf{z}}, \boldsymbol{\theta}) = \prod_{k=t}^T p(x_k|z_k, \boldsymbol{\theta})$ and $q(\bar{\mathbf{x}}) = \prod_{k=t}^T q(x_k)$. When we substitute a factor in the expectation term of the VFE (2) we write G instead of F for clarity.

Minimisation of the GFE maximises a mutual information between future observations and states [21]. The agent is then inclined to choose policies that resolve information about expected observations, leading to epistemic behaviour. A mathematical exploration of epistemic properties in CFFGs is available in [15].

In this paper we will view the p-substitution (2) as part of the optimisation constraints \mathcal{Q} . We then denote the p-substitution by a square bead in the CFFG, as drawn in Fig. 3 (right). As a convention, the square bead is drawn at the factor that is substituted [15].

4 General GFE-Based Message Updates

In the model for future states, the goal prior and observation model impose simultaneous constraints on the observation variable. In the corresponding CFFG, this configuration is modelled by two facing nodes. In this section we derive the general GFE-based message updates for a pair of facing nodes. We express the local optimisation problem as a Lagrangian. Using variational calculus we then derive local stationary solutions, from which we obtain general update expressions for GFE-based messages.

4.1 Goal and Observation Model

Here we define a generalised goal and observation model, which define simultaneous constraints on the observation variable x . The observation model $p(x|\mathbf{z}, \boldsymbol{\theta})$ consists of states \mathbf{z} and parameters $\boldsymbol{\theta}$. The goal prior extends to a goal model $\tilde{p}(x|\mathbf{w}, \boldsymbol{\phi})$, with states \mathbf{w} and parameters $\boldsymbol{\phi}$, expanding the range of applicability.

The CFFG of Fig. 4 draws the observation and goal model as two facing nodes. Crucially, from the perspective of the CFFG the role of these nodes in the bigger model is irrelevant, expanding the range of applicability beyond observation and goal models. Moreover, the facing nodes are contained by a composite structure that acts as a Markov blanket for communication with the remaining graph.

The CFFG of Fig. 4 also defines the free energy objective,

$$F[q] = \mathbb{E}_{q(x, \mathbf{z}, \boldsymbol{\theta}, \mathbf{w}, \boldsymbol{\phi})} \left[\log \frac{q(x, \mathbf{z}, \boldsymbol{\theta}, \mathbf{w}, \boldsymbol{\phi})}{p(x|\mathbf{z}, \boldsymbol{\theta})\tilde{p}(x|\mathbf{w}, \boldsymbol{\phi})} \right],$$

under local normalisation and marginalisation constraints, the imposed factorisation

$$q(x, \mathbf{z}, \boldsymbol{\theta}, \mathbf{w}, \boldsymbol{\phi}) \triangleq q(x)q(\mathbf{z})q(\boldsymbol{\theta})q(\mathbf{w})q(\boldsymbol{\phi}),$$

and p-substitution of

$$q(x) \rightarrow p(x|\mathbf{z}, \boldsymbol{\theta}),$$

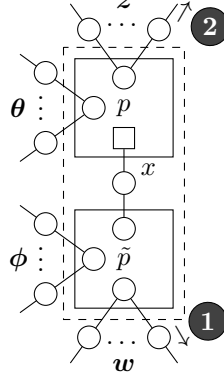


Figure 4: Explicit CFFG of two facing nodes with indicated p-substitution and messages.

in the expectation term.

4.2 Local Lagrangian

After substitution of the factorisation and applying the p-substitution to the local VFE objective, we obtain the local GFE,

$$G[q] = \mathbb{E}_{p(x|\mathbf{z}, \boldsymbol{\theta})q(\mathbf{z})q(\boldsymbol{\theta})q(\mathbf{w})q(\boldsymbol{\phi})} \left[\log \frac{q(x)q(\mathbf{z})q(\boldsymbol{\theta})q(\mathbf{w})q(\boldsymbol{\phi})}{p(x|\mathbf{z}, \boldsymbol{\theta})\tilde{p}(x|\mathbf{w}, \boldsymbol{\phi})} \right].$$

To find local stationary solutions to this GFE, we introduce Lagrange multipliers that enforce the normalisation and marginalisation constraints in \mathcal{Q} . The node-local Lagrangian then becomes

$$L[q] = G[q] + \sum_{a \in \mathcal{V}} \psi_a \left(\int q(\mathbf{s}_a) d\mathbf{s}_a - 1 \right) + \sum_{i \in \mathcal{E}} \psi_i \left(\int q(s_i) ds_i - 1 \right) + \sum_{a \in \mathcal{V}} \sum_{i \in \mathcal{E}(a)} \int \lambda_{ia}(s_i) \left(q(s_i) - \int q(\mathbf{s}_a) d\mathbf{s}_{a \setminus i} \right) ds_i, \quad (4)$$

with $s_i \in \{x, \mathbf{z}, \boldsymbol{\theta}, \mathbf{w}, \boldsymbol{\phi}\}$ a generic variable.

This Lagrangian is then optimised under a free-form variational density

$$q^* = \arg \min_q L[q],$$

for all individual factors in the variational distribution factorisation.

4.3 Local Stationary Solutions

We are now prepared to derive the stationary points of the node-local Lagrangian (4). We start by considering the node-local Lagrangian as a functional of the variational factor q_x .

Lemma 1. *Stationary points of $L[q]$ as a functional of q_x ,*

$$L[q_x] = G[q_x] + \psi_x \left[\int q(x) dx - 1 \right] + C_x, \quad (5)$$

where C_x collects all terms independent from q_x , are given by

$$q^*(x) = \mathbb{E}_{q(\mathbf{z})q(\boldsymbol{\theta})}[p(x|\mathbf{z}, \boldsymbol{\theta})]. \quad (6)$$

Proof. The proof is given by Appendix A.1. \square

Next, we derive the stationary points of (4) as a functional of $q_{\mathbf{z}}$. Note that, by symmetry, a similar result applies to $q_{\boldsymbol{\theta}}$.

Lemma 2. *Stationary points of $L[q]$ as a functional of $q_{\mathbf{z}}$,*

$$\begin{aligned} L[q_{\mathbf{z}}] &= G[q_{\mathbf{z}}] + \psi_{\mathbf{z}} \left[\int q_{\mathbf{z}}(\mathbf{z}) d\mathbf{z} - 1 \right] \\ &+ \sum_{i \in \mathcal{E}(\mathbf{z})} \int \lambda_{ip}(z_i) \left[q(z_i) - \int q_{\mathbf{z}}(\mathbf{z}) d\mathbf{z}_{\setminus i} \right] dz_i + C_{\mathbf{z}}, \end{aligned} \quad (7)$$

where $C_{\mathbf{z}}$ collects all terms independent from $q_{\mathbf{z}}$, are given by

$$q^*(\mathbf{z}) = \frac{\tilde{f}(\mathbf{z}) \prod_{z_i \in \mathbf{z}} \vec{\mu}(z_i)}{\int \tilde{f}(\mathbf{z}) \prod_{z_i \in \mathbf{z}} \vec{\mu}(z_i) d\mathbf{z}}, \quad (8)$$

with

$$\tilde{f}(\mathbf{z}) = \exp \left(\mathbb{E}_{p(x|\mathbf{z}, \boldsymbol{\theta})q(\boldsymbol{\theta})} \left[\log \frac{p(x|\mathbf{z}, \boldsymbol{\theta}) \tilde{f}(x)}{q(x)} \right] \right) \quad (9a)$$

$$\tilde{f}(x) = \exp(\mathbb{E}_{q(\mathbf{w})q(\phi)}[\log \tilde{p}(x|\mathbf{w}, \phi)]) . \quad (9b)$$

Proof. The proof is given by Appendix A.2. \square

Finally, we derive the stationary points of (4) with respect to $q_{\mathbf{w}}$. Again, by symmetry, a similar result follows for q_{ϕ} .

Lemma 3. *Stationary points of $L[q]$ as a functional of $q_{\mathbf{w}}$,*

$$\begin{aligned} L[q_{\mathbf{w}}] &= G[q_{\mathbf{w}}] + \psi_{\mathbf{w}} \left[\int q(\mathbf{w}) d\mathbf{w} - 1 \right] \\ &+ \sum_{i \in \mathcal{E}(\mathbf{w})} \int \lambda_{i\tilde{p}}(w_i) \left[q(w_i) - \int q(\mathbf{w}) d\mathbf{w}_{\setminus i} \right] dw_i + C_{\mathbf{w}}, \end{aligned} \quad (10)$$

where $C_{\mathbf{w}}$ collects all terms independent from $q_{\mathbf{w}}$, are given by

$$q^*(\mathbf{w}) = \frac{\tilde{f}(\mathbf{w}) \prod_{w_i \in \mathbf{w}} \vec{\mu}(w_i)}{\int \tilde{f}(\mathbf{w}) \prod_{w_i \in \mathbf{w}} \vec{\mu}(w_i) d\mathbf{w}}, \quad (11)$$

with

$$\tilde{f}(\mathbf{w}) = \exp(\mathbb{E}_{q(x|q(\phi))}[\log \tilde{p}(x|\mathbf{w}, \phi)]) . \quad (12)$$

Proof. The proof is given by Appendix A.3. \square

4.4 Message Updates

In this section we show that the stationary solutions of Sec. 4.3 correspond to the fixed points of a fixed-point iteration scheme. The corresponding messages are shown in Fig. 4. We first derive the update rule for message **1** on $w_j \in \mathbf{w}$. By symmetry, a similar result applies to $\phi_j \in \phi$.

Theorem 1. *Given the stationary points of the node-local Lagrangian $L[q]$, the stationary message $\overleftarrow{\mu}(w_j)$ corresponds to a fixed point of the iterations*

$$\overleftarrow{\mu}^{(n+1)}(w_j) = \int \tilde{f}(\mathbf{w}) \prod_{\substack{w_i \in \mathbf{w} \\ w_i \neq w_j}} \vec{\mu}^{(n)}(w_i) d\mathbf{w}_{\setminus j}, \quad (13)$$

with n an iteration index, and $\tilde{f}(\mathbf{w})$ given by (12).

Proof. The proof is given by Appendix B.1. \square

We now derive the update rule for message **2** on $z_j \in \mathbf{z}$ (Fig. 4), where we apply the same procedure as before. By symmetry, a similar result applies to $\theta_j \in \theta$.

Theorem 2. *Given the stationary points of the node-local Lagrangian $L[q]$, the stationary message $\overleftarrow{\mu}(z_j)$ corresponds to a fixed point of the iterations*

$$\overleftarrow{\mu}^{(n+1)}(z_j) = \int \tilde{f}(\mathbf{z}) \prod_{\substack{z_i \in \mathbf{z} \\ z_i \neq z_j}} \vec{\mu}^{(n)}(z_i) d\mathbf{z}_{\setminus j}, \quad (14)$$

with n an iteration index, and $\tilde{f}(\mathbf{z})$ given by (9),

Proof. The proof is given by Appendix B.2. \square

4.5 Convergence Considerations

While direct application of (14) works well in some cases, this message update may also yield algorithms for which the GFE actually diverges over iterations. This perhaps counter-intuitive effect then has major implications for the practical implementation of (14).

This divergence issue relates to a subtlety about what is actually proven by our theorems. While our theorems prove that the stationary messages correspond to fixed-points of the node-local Lagrangian, the theorems do not guarantee that iterations of the fixed-point equations actually converge to said fixed-points. In order to guarantee that updates approach the fixed-points, we derive an alternative message update rule for message ② below.

Corollary 1. *Given the stationary points of the node-local Lagrangian $L[q]$, the stationary message $\overleftarrow{\mu}(z_j)$ corresponds to*

$$\overleftarrow{\mu}(z_j) \propto \frac{\int q(\mathbf{z}; \nu^*) d\mathbf{z}_{\setminus j}}{\overrightarrow{\mu}(z_j)}, \quad (15)$$

with ν^* a solution to

$$q(\mathbf{z}; \nu) \stackrel{!}{=} \frac{\tilde{f}(\mathbf{z}; \nu) \prod_{z_i \in \mathbf{z}} \overrightarrow{\mu}(z_i)}{\int \tilde{f}(\mathbf{z}; \nu) \prod_{z_i \in \mathbf{z}} \overrightarrow{\mu}(z_i) d\mathbf{z}}, \quad (16)$$

where $q_{\mathbf{z}}$ is parameterised by statistics ν , and where $\tilde{f}(\mathbf{z}; \nu)$ is given by (9), with

$$q(x; \nu) = \mathbb{E}_{q(\mathbf{z}; \nu)q(\boldsymbol{\theta})}[p(x|\mathbf{z}, \boldsymbol{\theta})], \quad (17)$$

which is parameterised by ν through a recursive dependence on $q_{\mathbf{z}}$.

Proof. The proof is given by Appendix B.3. \square

The result of Corollary 1 avoids the possibly diverging fixed-point iterations of Theorem 2. For example, the optimal parameters ν^* can now be found through Newton's method.

5 Application to a Discrete-Variable Model

In this section we apply the general message update rules of Sec. 4.4 to a specific discrete-variable model that is often used in AIF practice. Using the general results we derive messages on this specific model.

5.1 Goal-Observation Submodel

As convention we use upright bold notation for vectors and matrices. We consider a discrete state $z \in \mathcal{Z}$ and observation variable $x \in \mathcal{X}$. To conveniently model

these variables with categorical distributions, we convert them to a one-hot representation, with $\mathbf{x} = \mathbf{e}_{\mathcal{X}}(x)$ the standard unit vector on \mathcal{X} with $x_i = 1$ at the index for x , and 0 otherwise. (And similar for \mathbf{z}). The notation $\text{Cat}(\mathbf{x}|\boldsymbol{\rho}) = \prod_i \rho_i^{x_i}$ then represents the categorical distribution on \mathbf{x} (one-hot) with probability vector $\boldsymbol{\rho}$. We relate the state and observation variables by transition probability matrix $\mathbf{A} \in \mathcal{X} \times \mathcal{Z}$. The columns of \mathbf{A} are normalised such that $\mathbf{A}\mathbf{z}$ represents a probability vector.

With notation in place, we define the observation model and goal prior for constrained submodel,

$$\begin{aligned} p(\mathbf{x}|\mathbf{z}, \mathbf{A}) &= \text{Cat}(\mathbf{x}|\mathbf{A}\mathbf{z}) \\ \tilde{p}(\mathbf{x}|\mathbf{c}) &= \text{Cat}(\mathbf{x}|\mathbf{c}) , \end{aligned}$$

as drawn in Fig. 5 (left).

5.2 GFE-Based Message Updates

The CFFG of Fig. 5 (left) defines the local GFE objective, with an incoming message $\mu_{\oplus}(\mathbf{z}) = \text{Cat}(\mathbf{z}|\mathbf{d})$. We denote by

$$\mathbf{h}(\mathbf{A}) = -\text{diag}(\mathbf{A}^T \log \mathbf{A}) ,$$

the vector of entropies of the columns of the conditional probability matrix \mathbf{A} .

As a notational convention, in this context we use an over-bar shorthand to denote an expectation, $\bar{\mathbf{z}} = \mathbb{E}_{q(\mathbf{z})}[\mathbf{z}]$. The table in Fig. 5 (right) summarises the resulting message updates and average energy, with

$$\begin{aligned} \boldsymbol{\xi}(\mathbf{A}) &= \mathbf{A}^T (\overline{\log \mathbf{c}} - \log(\overline{\mathbf{A}\bar{\mathbf{z}}})) - \mathbf{h}(\mathbf{A}) \\ \boldsymbol{\rho} &= \overline{\mathbf{A}^T (\overline{\log \mathbf{c}} - \log(\overline{\mathbf{A}\bar{\mathbf{z}}}))} - \overline{\mathbf{h}(\mathbf{A})} . \end{aligned}$$

The full derivations are available in Appendix C.

Unfortunately, message **3** does not express a (scaled) standard distribution type as a function of \mathbf{A} . Therefore we pass the log-message as a function directly and use importance sampling to evaluate expectations of $q(\mathbf{A})$ [1]. Estimation of the observation matrix through importance sampling thus renders GFE optimisation a stochastic procedure. As a result, the GFE may fluctuate over iterations. For policy selection, we therefore average the GFE over iterations, after a short burn-in period (ten iterations in this case).

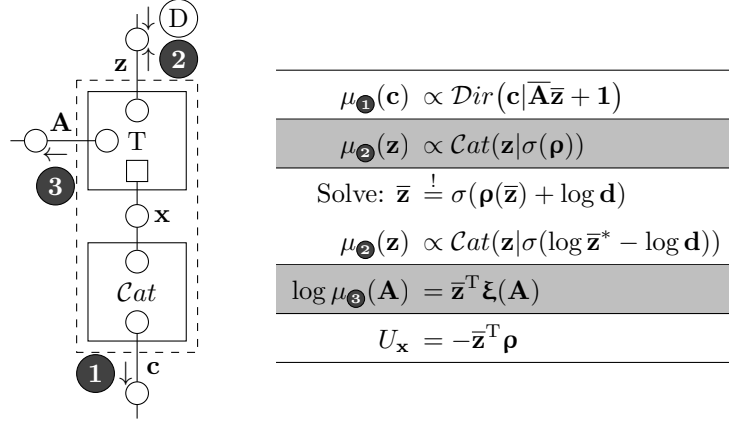


Figure 5: Discrete-variable submodel with indicated constraints (left) and message updates (right), with σ a softmax function. Updates for message two indicate the direct and indirect computation respectively.

5.3 Data-Constrained Message Updates

The message updates for a data-constrained VFE objective (Fig. 6, left) reduce to standard VMP updates (right), as derived by [28, App. A].

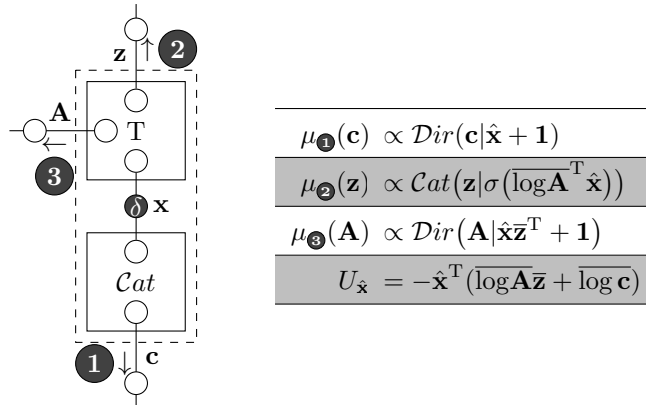


Figure 6: Discrete-variable submodel with data-constraint (left) and indicated message updates (right), with σ a softmax function and $\hat{\mathbf{x}}$ the (one-hot encoded) observation. Updates from [28, App. A].

6 Perception-Action Cycle

In this section we formulate a perception-action cycle that extends upon the GFE formulation of [21]. Specifically, we illustrate how the CFFG notation allows us to be explicit about local constraints. As a result, the perception-action cycle can now be visualised as a process that modifies constraints over time.

At the initial time $t = 1$ no observations are available, and we initialise the perception-action cycle with the CFFG of Fig. 7 (top). As actions are executed and observations become available, data-constraints replace the p-substitution on the observation variables (middle). When the time horizon is reached and all observations are available (bottom), inference corresponds with learning a posterior belief over parameters. This posterior can then be used as a prior in the next simulation trial. In line with [21], the perception-action cycle with time-dependent constraints thus unifies the tasks of perception, control and learning under a single GM and schedule. The experimental protocol is summarised in Algorithm 1, see also [29].

First, the **infer** step accepts the current model, constraints and past actions, and returns a collection of free energies that correspond with the allowed policies at time t . Naturally, at time $t = 1$ no past actions are available yet, and at time $t = T + 1$ all actions have been executed. In the latter case, the **infer** function returns the variational density for the parameters, which is used by the **update** step to update the prior statistics in the model. After the initial **infer** step, the **act** step accepts the collection of free energies and applies a strategy to select the best policy. In our case, we simply select the policy with lowest free energy. The first action of the policy is then returned, and executed in the environment by the **execute** step. The environment responds with a new observation, which

Algorithm 1 Experimental protocol for perception-action cycle.

Require: a generative model f_1 and a variational distribution with associated constraints $q \in \mathcal{Q}_1$

```

1: for  $s = 1$  to  $S$  do
2:   for  $t = 1$  to  $T$  do
3:      $\mathbf{G}_t = \text{infer}(f_s, \mathcal{Q}_t, \hat{\mathbf{u}})$  //infer free energies for selected policies
4:      $\hat{\mathbf{u}}_t = \text{act}(\mathbf{G}_t)$  //select an action
5:      $\text{execute}(\hat{\mathbf{u}}_t)$  //execute the action in the environment
6:      $\hat{x}_t = \text{observe}()$  //observe the resulting outcome
7:      $\mathcal{Q}_{t+1} = \text{slide}(\mathcal{Q}_t, \hat{x}_t)$  //update data-constraints
8:   end for
9:    $q_s^* = \text{infer}(f_s, \mathcal{Q}_{T+1}, \hat{\mathbf{u}})$  //learn parameters
10:   $f_{s+1} = \text{update}(f_s, q_s^*)$  //update prior statistics
11: end for
```

is returned by the **observe** step. At the end of the cycle, the **slide** step uses the observation to update the optimisation constraints.

This perception-action cycle lends itself particularly well for a reactive programming implementation. Namely, the GM and schedule remain, while the time-dependent constraints and associated update rules dynamically react to observations as they become available over time.

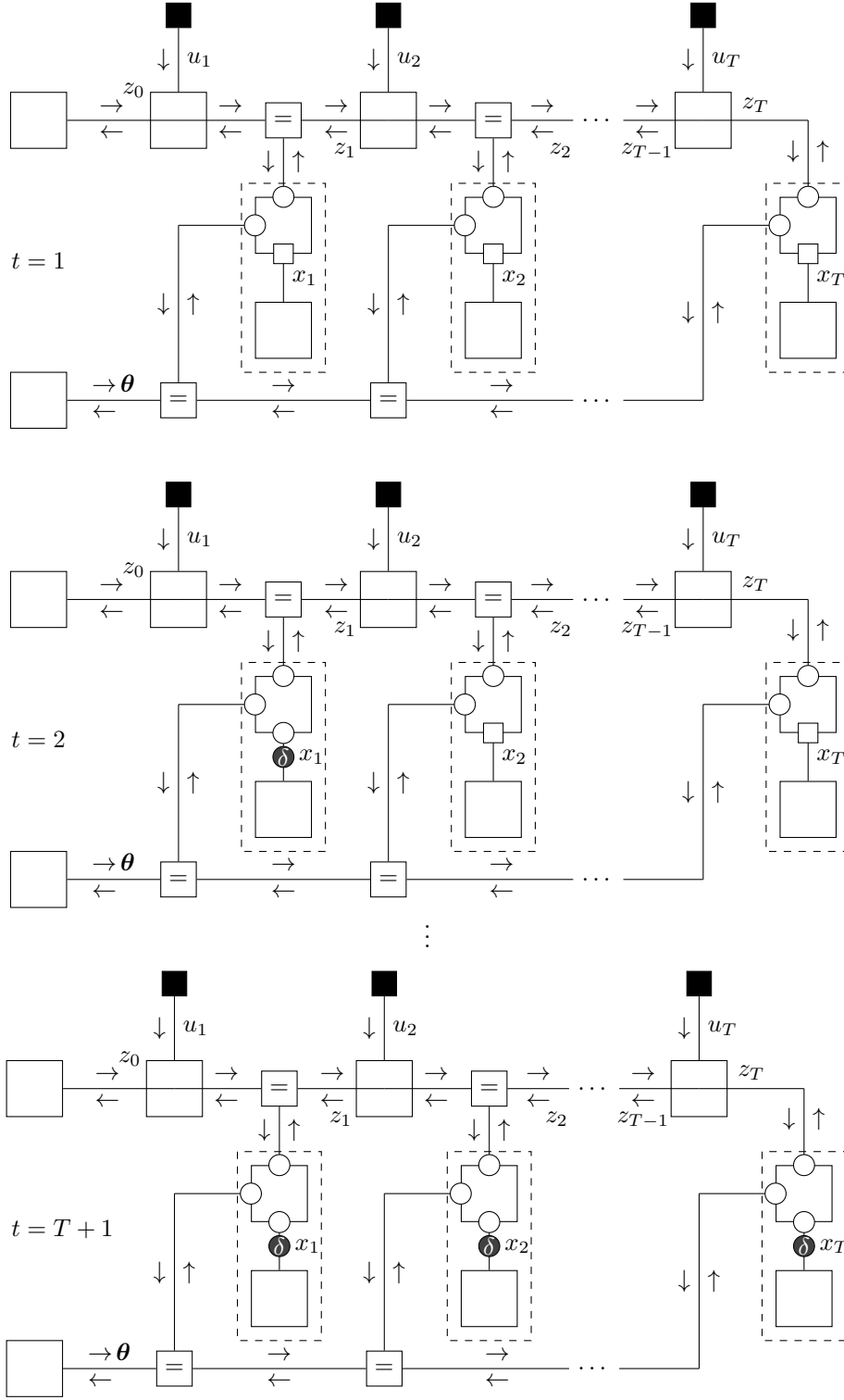


Figure 7: Unified inference procedure for learning, perception and control as observations become available over time.

7 Experimental Setting

In this section we describe a T-maze task that serves as a classical setting for investigating epistemic behaviour [10]. The setup closely follows the definitions in [30].

7.1 T-Maze Layout

The T-maze consists of four positions $\mathcal{P} = (O, C, L, R)$ as illustrated in Fig. 8. The agent starts at position O , with the objective to obtain a reward that is located either in arm L or arm R . The hidden reward location is represented by $\mathcal{R} = (RL, RR)$ for position L and R respectively. Visiting the cue position C reveals the reward location to the agent.

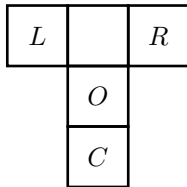


Figure 8: Layout of the T-maze with starting position O , cue position C and possible reward arms L and R .

The agent is allowed two moves ($T = 2$), and after each move the agent observes an outcome $\mathcal{O} = (CL, CR, RW, NR)$ that indicates

- CL : The reward is located in arm L ;
- CR : The reward is located in arm R ;
- RW : The reward is obtained;
- NR : No reward is obtained.

These outcomes stochastically relate to the agent position and reward location as listed in Table 3, with α the reward probability upon visiting the correct arm.

To ensure that the agent observes reward no more than once, a move to either reward arm is followed by a mandatory move back to the starting position (irrespective of whether reward was obtained or not). An epistemic agent would first visit the cue position and then move to the indicated reward position.

7.2 T-Maze Model Specification

Here we define a GM for the T-maze environment. The observation variables $x_k \in \mathcal{O} \times \mathcal{P}$ represent the outcome at the agent's position at time k (sixteen

\mathcal{P}	\mathcal{R}	CL	CR	RW	NR
O	RL	0.5	0.5	.	.
	RR	0.5	0.5	.	.
L	RL	.	.	α	$1 - \alpha$
	RR	.	.	$1 - \alpha$	α
R	RL	.	.	$1 - \alpha$	α
	RR	.	.	α	$1 - \alpha$
C	RL	1	.	.	.
	RR	.	1	.	.

Table 3: Probabilities for outcomes (\mathcal{O}) as related to agent position (\mathcal{P}) and reward position (\mathcal{R}).

possible combinations). An observation matrix \mathbf{A} then relates x_k to a state $z_k \in \mathcal{P} \times \mathcal{R}$. The state variable represents the agent position at time k , combined with the hidden reward position (eight possible combinations).

The control $u_k \in \mathcal{P}$ represents the agent’s desired next position (four possibilities). The control then selects the transition matrix \mathbf{B}_{u_k} .

As before, the GM represents categorical variables by one-hot encoded vectors. We will simulate the T-maze for S consecutive trials. The goal-constrained model for simulation s then becomes

$$f_s(\mathbf{x}, \mathbf{z}, \mathbf{A}|\mathbf{u}) = p(\mathbf{z}_0)p_s(\mathbf{A}) \prod_{k=1}^T p(\mathbf{x}_k|\mathbf{z}_k, \mathbf{A})p(\mathbf{z}_k|\mathbf{z}_{k-1}, \mathbf{u}_k)\tilde{p}(\mathbf{x}_k),$$

where the (empirical) parameter prior is indexed by trial number s .

We specify the sub-models,

$$\begin{aligned} p(\mathbf{z}_0) &= \text{Cat}(\mathbf{z}_0|\mathbf{d}) \\ p_s(\mathbf{A}) &= \text{Dir}(\mathbf{A}|\mathbf{A}_{s-1}) \\ p(\mathbf{x}_k|\mathbf{z}_k, \mathbf{A}) &= \text{Cat}(\mathbf{x}_k|\mathbf{A}\mathbf{z}_k) \\ p(\mathbf{z}_k|\mathbf{z}_{k-1}, \mathbf{u}_k) &= \text{Cat}(\mathbf{z}_k|\mathbf{B}_{u_k}\mathbf{z}_{k-1}) \\ \tilde{p}(\mathbf{x}_k) &= \text{Cat}(\mathbf{x}_k|\mathbf{c}), \end{aligned}$$

where the Dirichlet prior on the transition matrix assumes independent columns.

For the state prior we endow the agent with knowledge about its initial position, but ignorance about the reward position

$$\mathbf{d} = (1, 0, 0, 0)^T \otimes (0.5, 0.5)^T,$$

with \otimes the Kronecker product. Since the goal of the agent is to obtain reward, we define the goal prior statistic

$$\mathbf{c} = \sigma((0, 0, c, -c)^T \otimes (1, 1, 1, 1)^T),$$

with c the reward utility.

The prior for the transition matrix encodes the prior knowledge that position O does not offer any disambiguation, but the other positions might. Formally, \mathbf{A}_0 defines a block-diagonal matrix, with blocks

$$\mathbf{A}_{0,O} = \begin{pmatrix} 10 & 10 \\ 10 & 10 \\ \epsilon & \epsilon \\ \epsilon & \epsilon \end{pmatrix} \quad \mathbf{A}_{0,\{L,R,C\}} = \begin{pmatrix} 1 & \epsilon \\ \epsilon & 1 \\ \epsilon & \epsilon \\ \epsilon & \epsilon \end{pmatrix},$$

and $\epsilon = 0.1$ a relatively small value on all remaining entries, such that

$$\mathbf{A}_0 = \begin{pmatrix} \mathbf{A}_{0,O} & \epsilon & \epsilon & \epsilon \\ \epsilon & \mathbf{A}_{0,L} & \epsilon & \epsilon \\ \epsilon & \epsilon & \mathbf{A}_{0,R} & \epsilon \\ \epsilon & \epsilon & \epsilon & \mathbf{A}_{0,C} \end{pmatrix}.$$

Finally, the control-dependent transition matrices are defined as

$$\begin{aligned} \mathbf{B}_O &= \begin{pmatrix} 1 & 1 & 1 & 1 \\ 0 & 0 & 0 & 0 \\ 0 & 0 & 0 & 0 \\ 0 & 0 & 0 & 0 \end{pmatrix} \otimes \mathbf{I}_2 & \mathbf{B}_L &= \begin{pmatrix} 0 & 1 & 1 & 0 \\ 1 & 0 & 0 & 1 \\ 0 & 0 & 0 & 0 \\ 0 & 0 & 0 & 0 \end{pmatrix} \otimes \mathbf{I}_2 \\ \mathbf{B}_R &= \begin{pmatrix} 0 & 1 & 1 & 0 \\ 0 & 0 & 0 & 0 \\ 1 & 0 & 0 & 1 \\ 0 & 0 & 0 & 0 \end{pmatrix} \otimes \mathbf{I}_2 & \mathbf{B}_C &= \begin{pmatrix} 0 & 1 & 1 & 0 \\ 0 & 0 & 0 & 0 \\ 0 & 0 & 0 & 0 \\ 1 & 0 & 0 & 1 \end{pmatrix} \otimes \mathbf{I}_2, \end{aligned}$$

with \mathbf{I}_2 the 2×2 identity matrix. The CFFG for the T-maze is shown in Fig. 9.

8 Simulations

We set the reward probability $\alpha = 0.9$ and reward utility $c = 2$, and execute the perception-action cycle of Sec. 6 for $S = 100$ consecutive trials. Simulations are performed with the reactive message passing toolbox RxInfer [2]. The resulting minimum policy GFE over trials, grouped by time, is plotted in Fig. 10 (top left). It can be seen that the GFE decreases overall, as the agent improves its model of the environment. With an improved model better actions can be proposed, and the agent learns to first seek the clue and then visit the indicated reward arm.

The middle plots indicate whether the agent has observed a RW during a trial (on either move) which we designate as a win. We consider the trial a loss if the agent has failed to observe a RW on both moves. The free energy plot shows several spikes during the learning phase (top left, $t = 3$). These spikes coincide with unexpected losses (Fig. 10, middle left). Namely, after some moves the agent has learned to exploit the cue position C . However, even when the agent visits the indicated reward arm, an (unexpected) NR observation may still occur with probability $\alpha - 1$.

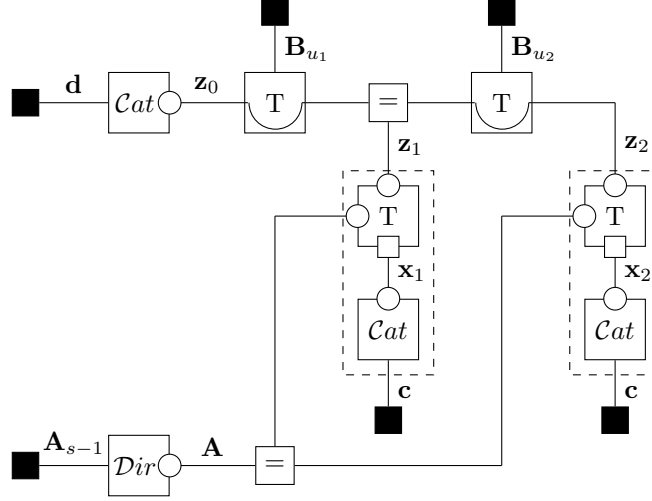


Figure 9: Constrained Forney-style factor graph for the T-maze.

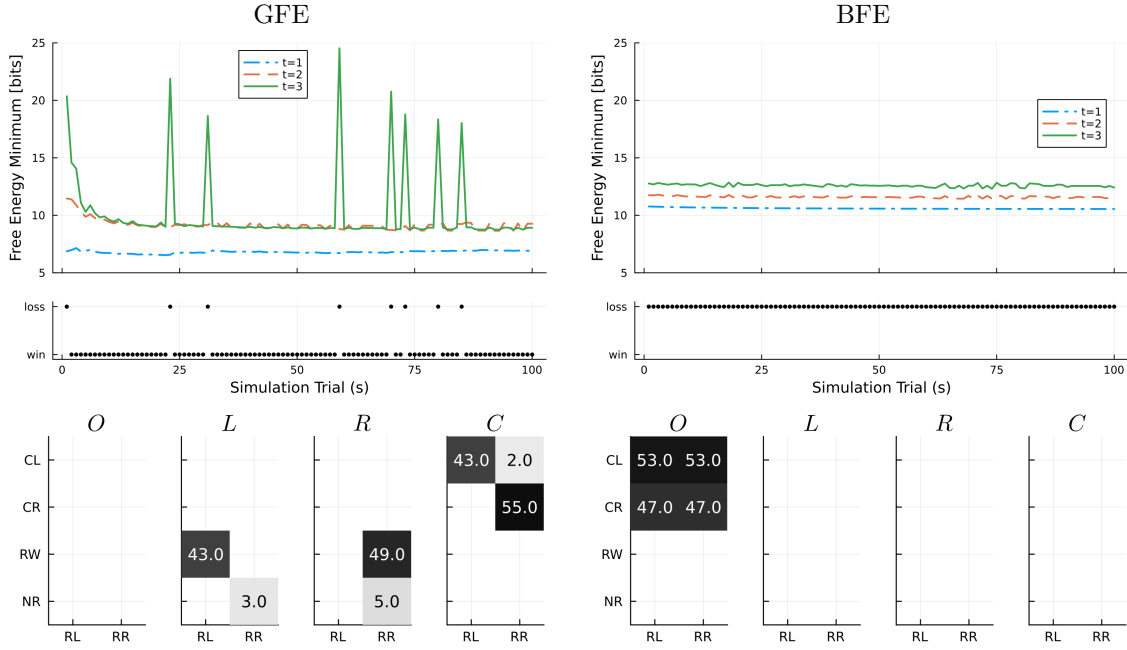


Figure 10: Generalised free energy over trials s as grouped by time t (top) with indicated win or loss (middle). A win indicates that a RW was observed on that trial (on either move). Bottom plots show learned statistics for the observation matrix $A_S - A_0$, as grouped per position.

After all trials have completed, we can inspect what the agent has learned. In Fig. 10 (bottom left) we plot the reinforced statistics $\mathbf{A}_S - \mathbf{A}_0$, as grouped per agent position. Each sub-plot then indicates the learned interaction between outcome and reward position at the indicated agent position. The GFE-based agent has confidently learned that position O offers disambiguation about the reward context, and that positions L and R offer a context-related reward RW (and sometimes NR). This knowledge then enables the agent to confidently pursue epistemic policies.

We compare the GFE-based agent with an agent that internalises an objective without substitution constraint. Specifically, in the CFFG of Fig. 9, the square that indicates a substitution constraint is replaced by a circle. This simple adjustment then reduces the GFE objective to a (structured) Bethe Free Energy (BFE) objective, which is known to lack epistemic qualities [25, 30]. We execute the same experimental protocol as before and plot the minimal free energies in Fig. 10 (top right).

The BFE-based reference agent fails to identify epistemic modes of behaviour. The specific choice of prior for the observation matrix prevents any extrinsic information (at least initially) from influencing policy selection. By lack of an epistemic drive, the BFE-based agent then sticks to policies that confirm its prior beliefs, without exploring possibilities to exploit available information in the T-maze environment (Fig. 10, bottom right).

Finally, we evaluate the reliability of the GFE-based agent by simulating $R = 100$ runs with $S = 30$ trials each. A histogram of the number of wins per run is plotted in Fig. 11 (left). This histogram suggests a bi-modal distribution with a large mass grouped to the right and a smaller mass in the middle. For reference, dashed curves indicates ideal performance for agents that already know \mathbf{A} from the start. For agents that must first learn \mathbf{A} , deviations from ideal performance are expected. The smaller middle mass then indicates that GFE optimisation offers no silver bullet for simulating fully successful epistemic agents. Namely, for some choices of initialisation, the GFE-based agent may still become stuck in local optima.

The win average per trial is plotted in Fig. 11 (right), which indicates that a GFE-based agent (on average) quickly learns to exploit the T-maze environment.

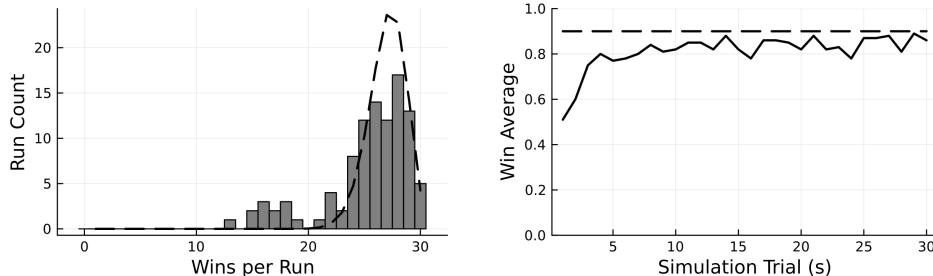


Figure 11: Aggregate results for $R = 100$ distinct runs with $S = 30$ trials each. Figures show the number of wins per run (left) and the win average per trial (right). Dashed curves indicate ideal performance of an agent with known \mathbf{A} for comparison.

9 Related Work

The Forney-style Factor Graph (FFG) notation was first introduced by [8]. The work of [19] offers a comprehensive introduction to message passing on FFGs in the context of signal processing and estimation.

The belief propagation algorithm was pioneered by [23], and was further formalised in terms of variational optimisation by [17, 33]. Variational Message Passing (VMP) was introduced by [32] and formulated in the context of FFGs by [6]. A more recent view on constrained free energy optimisation can be found in [34]. Furthermore, [27] offers a comprehensive overview of common constraints and resulting message passing updates on factor graphs.

Towards a message passing formulation of Active Inference (AIF), [21] proposed a Generalised Free Energy (GFE) objective, which incorporates prior beliefs on future outcomes as part of the Generative Model (GM). The current paper reformulates these ideas in a visual CFFG framework, which explicates the role of backward messages in GFE optimisation (see also our companion paper [15]). Inspired by [32], prior work by [4] derives variational message passing updates for AIF by augmenting variational message updates with an Expected Free Energy (EFE) term. In contrast, the current paper takes a constrained optimisation approach, augmenting the variational objective itself, and deriving message update expressions by variational optimisation.

Message passing formulations of AIF allow for modular extension to hierarchical structures. Temporal thickness in the context of message passing is explored by [7], which formulates deep temporal AIF by message passing on an FFG representation of a hierarchical GM. Implications of message passing in deep temporal models on neural connectivity are further explored by [12]. An operational framework and simulation environment for AIF by message passing on FFGs is described by [29].

Concerning epistemics and the exploration-exploitation trade-off, the pioneering work of [10] formally decomposes an EFE objective in constituent drivers for

behaviour, and motivates epistemic value from the perspective of maximizing information gain. A detailed view by [16] considers EFE minimisation in the context of linear Gaussian dynamical systems, and shows that AIF does not lead to purposeful explorative behaviour in this context.

Unfortunately, as our companion paper argues, the EFE optimisation viewpoint does not readily extend to message passing on free-form models [15]. Towards resolving this limitation, [25] formulated AIF as BFE optimisation, but also notes that the BFE lacks the crucial ambiguity-reducing component of the EFE that induces exploration. An alternative objective, the free energy of the expected future, was introduced by [20]. This objective includes the ambiguity-reducing component of the EFE and can be interpreted as the divergence from a biased to a veridical GM. An alternative AIF objective was proposed by [30], which considers epistemic behaviour from a constrained BFE perspective, and describes epistemic AIF by message passing on free-form GMs.

A biologically plausible view on message passing for AIF is described by [22], which combines the strengths of belief propagation and VMP to describe an alternative type of marginal message update.

10 Conclusions

This paper has taken a constraint-centric approach to synthetic Active Inference (AIF), and simulated a perception-action cycle through message passing derived from a single Generalised Free Energy (GFE) objective. Specifically, we have used a Constrained Forney-style Factor Graph (CFFG) visual representation to distinguish between the Generative Model (GM) and constraints on the Variational Free Energy (VFE).

Through constraint visualisations we have shown how the free energy objectives for perception, control and learning for AIF can be unified under a single GM specification and schedule, with time-dependent constraints.

The impact of our contributions lies with a modular and scalable formulation of synthetic AIF agents. Using variational calculus, we have derived general message update rules for GFE-based control. This allows for a modular approach to synthetic AIF, where custom message updates can be derived and reused across models. As an example we have derived GFE-based messages for a general configuration of two facing nodes, and applied these results to derive specific messages for a discrete-variable goal-observation submodel that is often used in AIF practice.

The general update rules allow for deriving GFE-based messages around alternative sub-models, including continuous-variable models and possibly chance-constrained models [31]. Additionally, the general message update results allows for a parametrised goal prior, which may be modelled by a secondary dynamical model [26].

Crucially, the local updates include novel backward messages that have not been expressed in traditional formulations of AIF. These backward messages ensure the unified optimisation of the full GFE objective, without resorting to

distinct schedules for state estimation and free energy evaluation. As limitations, we identified a possible convergence issue and possible complications in computing expectations. We also identified solutions to these limitations, in the form of an indirect message update using Newton’s method, and evaluating expectations through importance sampling, respectively.

With a CFFG representation and local message passing rules available, it becomes straightforward to mix and match constraints. We formulated an experimental protocol that unifies the tasks for perception, control and learning under a single GM and schedule. We simulated the perception-action cycle by a reactive programming implementation [2], where message updates dynamically react to time-dependent constraints as observations become available.

The presented T-maze simulations illustrate how synthetic AIF induces epistemic behaviour. Namely, where the GFE-based agent explores novel parameter settings and salient states, the reference Bethe Free Energy (BFE) based agent consistently fails to identify informative states in the environment.

In this paper we have adopted a purely engineering point-of-view, and we have not concerned ourselves with biological plausibility. Specifically, the derived message updates come with considerations about stability and non-standard expressions. Although we have engineered solutions to overcome these complications, it seems unlikely to us that the brain resorts to such strategies.

Acknowledgements

This research was made possible by funding from GN Hearing A/S. This work is part of the research programme Efficient Deep Learning with project number P16-25 project 5, which is (partly) financed by the Netherlands Organisation for Scientific Research (NWO).

We gratefully acknowledge stimulating discussions with the members of the BIASlab research group at the Eindhoven University of Technology, in particular Ismail Senoz, Bart van Erp and Dmitry Bagaev; and members of VERSES Research Lab, in particular Karl Friston, Chris Buckley, Conor Heins and Tim Verbelen. We also thank Mateus Joffily of the GATE-lab at le Centre National de la Recherche Scientifique for stimulating discussions.

References

- [1] Semih Akbayrak, Ivan Bocharov, and Bert de Vries. Extended Variational Message Passing for Automated Approximate Bayesian Inference. *Entropy*, 23(7):815, June 2021.
- [2] Dmitry Bagaev and Bert de Vries. Reactive Message Passing for Scalable Bayesian Inference. *arXiv:2112.13251 [cs]*, December 2021. arXiv: 2112.13251.

- [3] Ariel Caticha. Relative Entropy and Inductive Inference. *AIP Conference Proceedings*, 707:75–96, 2004. arXiv: physics/0311093.
- [4] Théophile Champion, Marek Grześ, and Howard Bowman. Realising Active Inference in Variational Message Passing: the Outcome-blind Certainty Seeker. *arXiv:2104.11798 [cs]*, April 2021. arXiv: 2104.11798.
- [5] Lancelot Da Costa, Thomas Parr, Noor Sajid, Sebastijan Veselic, Victorita Neacsu, and Karl Friston. Active inference on discrete state-spaces: a synthesis. *arXiv:2001.07203 [q-bio]*, January 2020. arXiv: 2001.07203.
- [6] Justin Dauwels. On Variational Message Passing on Factor Graphs. In *IEEE International Symposium on Information Theory*, pages 2546–2550, Nice, France, June 2007.
- [7] Bert de Vries and Karl J. Friston. A Factor Graph Description of Deep Temporal Active Inference. *Frontiers in Computational Neuroscience*, 11, 2017.
- [8] G.David Forney. Codes on graphs: normal realizations. *IEEE Transactions on Information Theory*, 47(2):520–548, February 2001.
- [9] Karl Friston, James Kilner, and Lee Harrison. A free energy principle for the brain. *Journal of Physiology, Paris*, 100(1-3):70–87, September 2006.
- [10] Karl Friston, Francesco Rigoli, Dimitri Ognibene, Christoph Mathys, Thomas Fitzgerald, and Giovanni Pezzulo. Active inference and epistemic value. *Cognitive Neuroscience*, 6(4):187–214, March 2015.
- [11] Karl J. Friston, Jean Daunizeau, and Stefan J. Kiebel. Reinforcement Learning or Active Inference? *PLoS ONE*, 4(7):e6421, July 2009.
- [12] Karl J Friston, Thomas Parr, and Bert de Vries. The graphical brain: belief propagation and active inference. *Network Neuroscience*, pages 1–78, June 2017.
- [13] Michael Kirchhoff, Thomas Parr, Ensor Palacios, Karl Friston, and Julian Kiverstein. The Markov blankets of life: autonomy, active inference and the free energy principle. *Journal of The Royal Society Interface*, 15(138):20170792, January 2018.
- [14] Daphne Koller and Nir Friedman. *Probabilistic graphical models: principles and techniques*. MIT press, 2009.
- [15] Magnus Koudahl, Thijs van de Laar, and Bert De Vries. Realising Synthetic Active Inference Agents, Part I: Epistemic Objectives and Graphical Specification Language. *In preparation*.
- [16] Magnus T. Koudahl, Wouter M. Kouw, and Bert de Vries. On Epistemics in Expected Free Energy for Linear Gaussian State Space Models. *Entropy*, 23(12):1565, 2021. Publisher: MDPI.

- [17] Frank R. Kschischang, Brendan J. Frey, and H.-A. Loeliger. Factor graphs and the sum-product algorithm. *IEEE Transactions on information theory*, 47(2):498–519, 2001.
- [18] Hans-Andrea Loeliger. An introduction to factor graphs. *Signal Processing Magazine, IEEE*, 21(1):28–41, January 2004.
- [19] Hans-Andrea Loeliger. Factor Graphs and Message Passing Algorithms – Part 1: Introduction, 2007. http://www.crm.sns.it/media/course/1524/Loeliger_A.pdf, last accessed on 3-4-2019.
- [20] Beren Millidge, Alexander Tschantz, and Christopher L. Buckley. Whence the Expected Free Energy? *arXiv preprint arXiv:2004.08128*, 2020.
- [21] Thomas Parr and Karl J. Friston. Generalised free energy and active inference. *Biological cybernetics*, 113(5):495–513, 2019. Publisher: Springer.
- [22] Thomas Parr, Dimitrije Markovic, Stefan J. Kiebel, and Karl J. Friston. Neuronal message passing using Mean-field, Bethe, and Marginal approximations. *Scientific Reports*, 9(1):1889, December 2019.
- [23] Judea Pearl. Reverend Bayes on Inference Engines: A Distributed Hierarchical Approach. In *Proceedings of the Second AAAI Conference on Artificial Intelligence*, AAAI’82, pages 133–136, Pittsburgh, Pennsylvania, 1982. AAAI Press.
- [24] Christoph Reller. *State-Space Methods in Statistical Signal Processing: New Ideas and Applications*. PhD thesis, ETH Zurich, 2012.
- [25] Sarah Schwöbel, Stefan Kiebel, and Dimitrije Marković. Active Inference, Belief Propagation, and the Bethe Approximation. *Neural Computation*, 30(9):2530–2567, September 2018.
- [26] Eli Sennesh, Jordan Theriault, Jan-Willem van de Meent, Lisa Feldman Barrett, and Karen Quigley. Deriving time-averaged active inference from control principles, August 2022. arXiv:2208.10601 [cs, eess, q-bio, stat].
- [27] İsmail Şenöz, Thijs van de Laar, Dmitry Bagaev, and Bert de Vries. Variational Message Passing and Local Constraint Manipulation in Factor Graphs. *Entropy*, 23(7):807, July 2021. Publisher: Multidisciplinary Digital Publishing Institute.
- [28] Thijs van de Laar. *Automated Design of Bayesian Signal Processing Algorithms*. PhD thesis, Eindhoven University of Technology, Eindhoven, The Netherlands, 2019.
- [29] Thijs van de Laar and Bert de Vries. Simulating Active Inference Processes by Message Passing. *Frontiers in Robotics and AI*, 6:20, 2019.

- [30] Thijs van de Laar, Magnus Koudahl, Bart van Erp, and Bert de Vries. Active Inference and Epistemic Value in Graphical Models. *Frontiers in Robotics and AI*, 9, 2022.
- [31] Thijs van de Laar, Ismail Şenöz, Ayça Özçelikkale, and Henk Wymeersch. Chance-Constrained Active Inference. *arXiv preprint arXiv:2102.08792*, 2021.
- [32] John Winn and Christopher M. Bishop. Variational Message Passing. *Journal of Machine Learning Research*, 6(23):661–694, 2005.
- [33] Jonathan S. Yedidia. Understanding Belief Propagation and its Generalizations. November 2001.
- [34] Dan Zhang, Wenjin Wang, Gerhard Fettweis, and Xiqi Gao. Unifying Message Passing Algorithms Under the Framework of Constrained Bethe Free Energy Minimization. *arXiv:1703.10932 [cs, math]*, March 2017. arXiv: 1703.10932.

A Proofs of Local Stationary Solutions in Section 4.3

This section derives the stationary points of a local GFE constrained objective, as defined by Fig. 4.

A.1 Proof of Lemma 1

Proof. Writing out the terms in the Lagrangian and simplifying, we obtain

$$L[q_x] = \mathbb{E}_{p(x|\mathbf{z}, \boldsymbol{\theta})q(\mathbf{z})q(\boldsymbol{\theta})}[\log q(x)] + \psi_x \left[\int q(x) dx - 1 \right] + C_x.$$

The functional derivative then becomes

$$\frac{\delta L}{\delta q_x} = \frac{\mathbb{E}_{q(\mathbf{z})q(\boldsymbol{\theta})}[p(x|\mathbf{z}, \boldsymbol{\theta})]}{q(x)} + \psi_x \stackrel{!}{=} 0.$$

Solving this equation for q_x results in (6). \square

A.2 Proof of Lemma 2

Proof. Writing out the Lagrangian, we obtain

$$\begin{aligned} L[q_{\mathbf{z}}] &= \mathbb{E}_{p(x|\mathbf{z}, \boldsymbol{\theta})q(\mathbf{z})q(\boldsymbol{\theta})q(\mathbf{w})q(\boldsymbol{\phi})} \left[\log \frac{q(x)}{p(x|\mathbf{z}, \boldsymbol{\theta})\tilde{p}(x|\mathbf{w}, \boldsymbol{\phi})} \right] + \mathbb{E}_{q(\mathbf{z})}[\log q(\mathbf{z})] \\ &\quad + \psi_{\mathbf{z}} \left[\int q(\mathbf{z}) d\mathbf{z} - 1 \right] + \sum_{i \in \mathcal{E}(\mathbf{z})} \int \lambda_{ip}(z_i) \left[q(z_i) - \int q(\mathbf{z}) d\mathbf{z}_{\setminus i} \right] dz_i + C_{\mathbf{z}}. \end{aligned}$$

The functional derivative then becomes

$$\begin{aligned} \frac{\delta L}{\delta q_{\mathbf{z}}} &= \mathbb{E}_{p(x|\mathbf{z}, \boldsymbol{\theta})q(\boldsymbol{\theta})q(\mathbf{w})q(\boldsymbol{\phi})} \left[\log \frac{q(x)}{p(x|\mathbf{z}, \boldsymbol{\theta})\tilde{p}(x|\mathbf{w}, \boldsymbol{\phi})} \right] + \log q(\mathbf{z}) + 1 + \psi_{\mathbf{z}} - \sum_{i \in \mathcal{E}(\mathbf{z})} \lambda_{ip}(z_i) \\ &= \mathbb{E}_{p(x|\mathbf{z}, \boldsymbol{\theta})q(\boldsymbol{\theta})} \left[\log \frac{q(x)}{p(x|\mathbf{z}, \boldsymbol{\theta})\tilde{f}(x)} \right] + \log q(\mathbf{z}) - \sum_{i \in \mathcal{E}(\mathbf{z})} \lambda_{ip}(z_i) + Z_{\mathbf{z}} \\ &= -\log \tilde{f}(\mathbf{z}) + \log q(\mathbf{z}) - \sum_{i \in \mathcal{E}(\mathbf{z})} \lambda_{ip}(z_i) + Z_{\mathbf{z}}, \end{aligned}$$

where $Z_{\mathbf{z}}$ absorbs all terms independent of \mathbf{z} , and with $\tilde{f}(\mathbf{z})$ and $\tilde{f}(x)$ given by (9a) and (9b) respectively.

Setting to zero and solving for $q_{\mathbf{z}}$, we obtain

$$\log q^*(\mathbf{z}) = \log \tilde{f}(\mathbf{z}) + \sum_{i \in \mathcal{E}(\mathbf{z})} \lambda_{ip}(z_i) - Z_{\mathbf{z}}.$$

Exponentiating on both sides, identifying $\vec{\mu}(z_i) = \exp \lambda_{ip}(z_i)$, and normalizing then results in (8). \square

A.3 Proof of Lemma 3

Proof. Writing out the Lagrangian, we obtain

$$\begin{aligned} L[q_{\mathbf{w}}] &= \mathbb{E}_{p(x|\mathbf{z}, \boldsymbol{\theta})q(\mathbf{z})q(\boldsymbol{\theta})q(\mathbf{w})q(\boldsymbol{\phi})} \left[\log \frac{q(x)}{p(x|\mathbf{z}, \boldsymbol{\theta})\tilde{p}(x|\mathbf{w}, \boldsymbol{\phi})} \right] + \mathbb{E}_{q(\mathbf{z})} [\log q(\mathbf{z})] \\ &\quad + \psi_{\mathbf{w}} \left[\int q(\mathbf{w}) d\mathbf{w} - 1 \right] + \sum_{i \in \mathcal{E}(\mathbf{w})} \int \lambda_{i\tilde{p}}(w_i) \left[q(w_i) - \int q(\mathbf{w}) d\mathbf{w}_{\setminus i} \right] dw_i + C_{\mathbf{w}}. \end{aligned}$$

The functional derivative then becomes

$$\begin{aligned} \frac{\delta L}{\delta q_{\mathbf{w}}} &= \mathbb{E}_{p(x|\mathbf{z}, \boldsymbol{\theta})q(\mathbf{z})q(\boldsymbol{\theta})q(\boldsymbol{\phi})} \left[\log \frac{q(x)}{p(x|\mathbf{z}, \boldsymbol{\theta})\tilde{p}(x|\mathbf{w}, \boldsymbol{\phi})} \right] + \log q(\mathbf{w}) + 1 + \psi_{\mathbf{w}} - \sum_{i \in \mathcal{E}(\mathbf{w})} \lambda_{i\tilde{p}}(w_i) \\ &= -\mathbb{E}_{p(x|\mathbf{z}, \boldsymbol{\theta})q(\mathbf{z})q(\boldsymbol{\theta})q(\boldsymbol{\phi})} [\log \tilde{p}(x|\mathbf{w}, \boldsymbol{\phi})] + \log q(\mathbf{w}) - \sum_{i \in \mathcal{E}(\mathbf{w})} \lambda_{i\tilde{p}}(w_i) + Z_{\mathbf{w}} \\ &= -\mathbb{E}_{q(x)q(\boldsymbol{\phi})} [\log \tilde{p}(x|\mathbf{w}, \boldsymbol{\phi})] + \log q(\mathbf{w}) - \sum_{i \in \mathcal{E}(\mathbf{w})} \lambda_{i\tilde{p}}(w_i) + Z_{\mathbf{w}} \\ &= -\log \tilde{f}(\mathbf{w}) + \log q(\mathbf{w}) - \sum_{i \in \mathcal{E}(\mathbf{w})} \lambda_{i\tilde{p}}(w_i) + Z_{\mathbf{w}} \end{aligned}$$

where $Z_{\mathbf{w}}$ absorbs all terms independent of \mathbf{w} , the second-to-last step uses the result of (6), and where $\tilde{f}(\mathbf{w})$ is given by (12).

Setting to zero and solving for $q_{\mathbf{w}}$, we obtain

$$\log q^*(\mathbf{w}) = \log \tilde{f}(\mathbf{w}) + \sum_{i \in \mathcal{E}(\mathbf{w})} \lambda_{i\tilde{p}}(w_i) - Z_{\mathbf{w}}.$$

Exponentiating on both sides, identifying $\vec{\mu}(w_i) = \exp \lambda_{i\tilde{p}}(w_i)$, and normalizing results in (11). \square

B Proofs of Message Update Expressions in Section 4.4

B.1 Proof of Theorem 1

Proof. Firstly, Lemma 3 provides us with the stationary solutions to $L[q]$ as a functional of $q_{\mathbf{w}}$. Secondly, the stationary solution of $L[q]$ as a functional of the edge-local variational distribution $q_j(w_j)$, defined as

$$\begin{aligned} L[q_j] &= H[q_j] + \psi_j \left[\int q(w_j) dz_j - 1 \right] \\ &\quad + \sum_{a \in \mathcal{V}(j)} \int \lambda_{ja}(w_j) \left[q(w_j) - \int q(\mathbf{w}) d\mathbf{w}_{\setminus j} \right] dw_j + C_j, \end{aligned}$$

where C_j absorbs all terms independent of q_j , directly follows from [27, Lemma 2], as

$$q^*(w_j) = \frac{\overrightarrow{\mu}(w_j)\overleftarrow{\mu}(w_j)}{\int \overrightarrow{\mu}(w_j)\overleftarrow{\mu}(w_j)dw_j}.$$

We then apply the marginalisation constraint on the edge- and node-local variational distributions

$$q^*(w_j) = \int q^*(\mathbf{w}) d\mathbf{w}_{\setminus j}.$$

Substituting the stationary solutions we can directly apply [27, Theorem 2]. It then follows that fixed points of (13) correspond to stationary solutions of $L[q]$. \square

The notation $\mu_{\bullet}(w_j) = \overleftarrow{\mu}^{(n+1)}(w_j)$ then conveniently represents the recursive message update schedule.

B.2 Proof of Theorem 2

Proof. We follow the same procedure as before. Firstly, Lemma 2 provides us with the stationary solutions of $L[q]$ as a functional of z_j . Secondly, the Lagrangian as a functional of $q_j(z_j)$ is then constructed as

$$\begin{aligned} L[q_j] &= H[q_j] + \psi_j \left[\int q(z_j) dz_j - 1 \right] \\ &+ \sum_{a \in \mathcal{V}(j)} \int \lambda_{ja}(z_j) \left[q(z_j) - \int q(\mathbf{z}) d\mathbf{z}_{\setminus j} \right] dz_j + C_j, \end{aligned}$$

where C_j absorbs all terms independent of q_j . The stationary solution again follows from [27, Lemma 2],

$$q^*(z_j) = \frac{\overrightarrow{\mu}(z_j)\overleftarrow{\mu}(z_j)}{\int \overrightarrow{\mu}(z_j)\overleftarrow{\mu}(z_j)dz_j}.$$

From the marginalisation constraint

$$q^*(z_j) = \int q^*(\mathbf{z}) d\mathbf{z}_{\setminus j},$$

we can again directly apply [27, Theorem 2], from which it follows that fixed points of (14) correspond to stationary solutions of $L[q]$. \square

In the schedule, the fixed-point iteration is then represented by $\mu_{\bullet}(z_j) = \overleftarrow{\mu}^{(n+1)}(z_j)$.

B.3 Proof of Corollary 1

Proof. From the marginalisation constraint we obtain (15). We then parameterise $q_{\mathbf{z}}$ with statistics ν and substitute (8), (9) and (6) to obtain a recursive dependence on ν . \square

C Derivations of Message Updates in Figure 5

Here we derive the message updates for the discrete-variable submodel of Fig. 5. To streamline the derivations of we first derive some intermediate results.

C.1 Intermediate Results

First we express the log-observation model,

$$\begin{aligned}\log p(\mathbf{x}|\mathbf{z}, \mathbf{A}) &= \log \text{Cat}(\mathbf{x}|\mathbf{A}\mathbf{z}) \\ &= \sum_j \sum_k x_j \log(A_{jk}) z_k \\ &= \mathbf{x}^T \log(\mathbf{A})\mathbf{z},\end{aligned}$$

where the final logarithm is taken element-wise.

Then, from (6),

$$\begin{aligned}\log q(\mathbf{x}) &= \log (\mathbb{E}_{q(\mathbf{z})q(\mathbf{A})}[p(\mathbf{x}|\mathbf{z}, \boldsymbol{\theta})]) \\ &= \log (\mathbb{E}_{q(\mathbf{z})q(\mathbf{A})}[\text{Cat}(\mathbf{x}|\mathbf{A}\mathbf{z})]) \\ &\approx \log \text{Cat}(\mathbf{x}|\overline{\mathbf{A}\mathbf{z}}) \\ &= \mathbf{x}^T \log(\overline{\mathbf{A}\mathbf{z}}),\end{aligned}$$

Where we used a tentative decision approximation to compute the expectations with respect to $q(\mathbf{A}) \stackrel{!}{=} \delta(\mathbf{A} - \overline{\mathbf{A}})$.

Next, from (9),

$$\begin{aligned}\log \tilde{f}(\mathbf{x}) &= \mathbb{E}_{q(\mathbf{c})}[\log \tilde{p}(\mathbf{x}|\mathbf{c})] \\ &= \mathbb{E}_{q(\mathbf{c})}[\log \text{Cat}(\mathbf{x}|\mathbf{c})] \\ &= \mathbb{E}_{q(\mathbf{c})}[\mathbf{x}^T \log \mathbf{c}] \\ &= \mathbf{x}^T \overline{\log \mathbf{c}}.\end{aligned}$$

Combining these results, from (9),

$$\begin{aligned}
\log \tilde{f}(\mathbf{z}) &= \mathbb{E}_{p(\mathbf{x}|\mathbf{z}, \mathbf{A})q(\mathbf{A})} \left[\log \frac{p(\mathbf{x}|\mathbf{z}, \mathbf{A})\tilde{f}(\mathbf{x})}{q(\mathbf{x})} \right] \\
&= \mathbb{E}_{p(\mathbf{x}|\mathbf{z}, \mathbf{A})q(\mathbf{A})} [\mathbf{x}^T \log(\mathbf{A})\mathbf{z} + \mathbf{x}^T \overline{\log \mathbf{c}} - \mathbf{x}^T \log(\overline{\mathbf{A}\mathbf{z}})] \\
&= \mathbb{E}_{q(\mathbf{A})} [(\mathbf{A}\mathbf{z})^T \log(\mathbf{A})\mathbf{z} + (\mathbf{A}\mathbf{z})^T \overline{\log \mathbf{c}} - (\mathbf{A}\mathbf{z})^T \log(\overline{\mathbf{A}\mathbf{z}})] \\
&= \mathbb{E}_{q(\mathbf{A})} [\mathbf{z}^T \text{diag}(\mathbf{A}^T \log \mathbf{A}) + (\mathbf{A}\mathbf{z})^T \overline{\log \mathbf{c}} - (\mathbf{A}\mathbf{z})^T \log(\overline{\mathbf{A}\mathbf{z}})] \\
&= \mathbb{E}_{q(\mathbf{A})} [-\mathbf{z}^T \mathbf{h}(\mathbf{A}) + (\mathbf{A}\mathbf{z})^T \overline{\log \mathbf{c}} - (\mathbf{A}\mathbf{z})^T \log(\overline{\mathbf{A}\mathbf{z}})] \\
&= -\mathbf{z}^T \overline{\mathbf{h}(\mathbf{A})} + (\overline{\mathbf{A}\mathbf{z}})^T \overline{\log \mathbf{c}} - (\overline{\mathbf{A}\mathbf{z}})^T \log(\overline{\mathbf{A}\mathbf{z}}) \\
&= \mathbf{z}^T \boldsymbol{\rho},
\end{aligned}$$

with

$$\boldsymbol{\rho} = \overline{\mathbf{A}}^T (\overline{\log \mathbf{c}} - \log(\overline{\mathbf{A}\mathbf{z}})) - \overline{\mathbf{h}(\mathbf{A})}, \quad (18)$$

and

$$\mathbf{h}(\mathbf{A}) = -\text{diag}(\mathbf{A}^T \log \mathbf{A}),$$

the entropies of the columns of matrix \mathbf{A} .

With these results we can derive the local GFE and messages.

C.2 Average Energy

$$\begin{aligned}
U_{\mathbf{x}}[q] &= \mathbb{E}_{p(\mathbf{x}|\mathbf{z}, \mathbf{A})q(\mathbf{z})q(\mathbf{A})q(\mathbf{c})} \left[\log \frac{q(\mathbf{x})}{p(\mathbf{x}|\mathbf{z}, \mathbf{A})\tilde{p}(\mathbf{x}|\mathbf{c})} \right] \\
&= -\mathbb{E}_{p(\mathbf{x}|\mathbf{z}, \mathbf{A})q(\mathbf{z})q(\mathbf{A})} \left[\log \frac{p(\mathbf{x}|\mathbf{z}, \mathbf{A})\tilde{f}(\mathbf{x})}{q(\mathbf{x})} \right] \\
&= -\mathbb{E}_{q(\mathbf{z})} [\log \tilde{f}(\mathbf{z})] \\
&= -\overline{\mathbf{z}}^T \boldsymbol{\rho},
\end{aligned}$$

with $\boldsymbol{\rho}$ given by (18).

C.3 Message ①

We apply the result of Theorem 1 and express the downward message,

$$\begin{aligned}
\log \mu_{\textcircled{1}}(\mathbf{c}) &= \log \tilde{f}(\mathbf{c}) \\
&= \mathbb{E}_{q(\mathbf{x})} [\log \tilde{p}(\mathbf{x}|\mathbf{c})] \\
&= \mathbb{E}_{q(\mathbf{x})} [\mathbf{x}^T \log \mathbf{c}] \\
&= (\overline{\mathbf{A}\mathbf{z}})^T \log \mathbf{c}.
\end{aligned}$$

Exponentiation on both sides then yields

$$\mu_{\textcircled{1}}(\mathbf{c}) \propto \mathcal{Dir}(\mathbf{c}|\overline{\mathbf{A}\mathbf{z}} + \mathbf{1}).$$

C.4 Direct Result for Message ②

Here we apply the result of Theorem 2 to directly compute the backward message for the state. As explained before, this update may lead to diverging FE for some algorithms.

$$\begin{aligned}\log \mu_{\bullet}(\mathbf{z}) &= \log \tilde{f}(\mathbf{z}) \\ &= \mathbf{z}^T \boldsymbol{\rho},\end{aligned}$$

with $\boldsymbol{\rho}$ given by (18). Exponentiation on both sides then yields

$$\mu_{\bullet}(\mathbf{z}) \propto \text{Cat}(\mathbf{z}|\sigma(\boldsymbol{\rho})),$$

with σ the softmax function.

C.5 Indirect Result for Message ②

Here we apply the result of Corollary 1. We set the statistic $\nu = \bar{\mathbf{z}}$, assume message ① (proportionally) Categorical, and use (16) to express

$$\begin{aligned}\log q(\mathbf{z}; \bar{\mathbf{z}}) &= \log \tilde{f}(\mathbf{z}; \bar{\mathbf{z}}) + \log \mu_{\oplus}(\mathbf{z}) + C_{\mathbf{z}} \\ &= \mathbf{z}^T \boldsymbol{\rho}(\bar{\mathbf{z}}) + \mathbf{z}^T \log \mathbf{d} + C_{\mathbf{z}},\end{aligned}$$

with $\boldsymbol{\rho}(\bar{\mathbf{z}})$ given by (18), where the circular dependence on $\bar{\mathbf{z}}$ has been made explicit.

Exponentiating on both sides and normalizing, we obtain

$$\begin{aligned}q(\mathbf{z}; \bar{\mathbf{z}}) &= \text{Cat}(\mathbf{z}|\bar{\mathbf{z}}), \text{ with} \\ \bar{\mathbf{z}} &= \sigma(\boldsymbol{\rho}(\bar{\mathbf{z}}) + \log \mathbf{d}),\end{aligned}\tag{19}$$

and σ the softmax function.

We then approach this equation as a root-finding problem, and use Newton's method to find an $\bar{\mathbf{z}}^*$ that solves for (19). We can then compute the backward message through (15), as

$$\begin{aligned}\mu_{\bullet}(\mathbf{z}) &\propto q(\mathbf{z}; \bar{\mathbf{z}}^*) / \mu_{\oplus}(\mathbf{z}) \\ &= \text{Cat}(\mathbf{z}|\bar{\mathbf{z}}^*) / \text{Cat}(\mathbf{z}|\mathbf{d}) \\ &\propto \text{Cat}(\mathbf{z}|\sigma(\log \bar{\mathbf{z}}^* - \log \mathbf{d})).\end{aligned}$$

C.6 Direct Result for Message ③

Here we apply the result of Theorem 2 and use the symmetry between \mathbf{z} and \mathbf{A} to directly compute the backward message for the state, as

$$\begin{aligned}
\log \mu_{\textcircled{3}}(\mathbf{A}) &= \mathbb{E}_{p(\mathbf{x}|\mathbf{z}, \mathbf{A})q(\mathbf{z})} \left[\log \frac{p(\mathbf{x}|\mathbf{z}, \mathbf{A})\tilde{f}(\mathbf{x})}{q(\mathbf{x})} \right] \\
&= \mathbb{E}_{p(\mathbf{x}|\mathbf{z}, \mathbf{A})q(\mathbf{z})} [\mathbf{x}^T \log(\mathbf{A})\mathbf{z} + \mathbf{x}^T \overline{\log \mathbf{c}} - \mathbf{x}^T \log(\overline{\mathbf{A}\mathbf{z}})] \\
&= \mathbb{E}_{q(\mathbf{z})} [(\mathbf{A}\mathbf{z})^T \log(\mathbf{A})\mathbf{z} + (\mathbf{A}\mathbf{z})^T \overline{\log \mathbf{c}} - (\mathbf{A}\mathbf{z})^T \log(\overline{\mathbf{A}\mathbf{z}})] \\
&= \mathbb{E}_{q(\mathbf{z})} [\mathbf{z}^T \text{diag}(\mathbf{A}^T \log \mathbf{A}) + (\mathbf{A}\mathbf{z})^T \overline{\log \mathbf{c}} - (\mathbf{A}\mathbf{z})^T \log(\overline{\mathbf{A}\mathbf{z}})] \\
&= \mathbb{E}_{q(\mathbf{z})} [-\mathbf{z}^T \mathbf{h}(\mathbf{A}) + (\mathbf{A}\mathbf{z})^T \overline{\log \mathbf{c}} - (\mathbf{A}\mathbf{z})^T \log(\overline{\mathbf{A}\mathbf{z}})] \\
&= \bar{\mathbf{z}}^T \boldsymbol{\xi}(\mathbf{A}),
\end{aligned}$$

with

$$\boldsymbol{\xi}(\mathbf{A}) = \mathbf{A}^T (\overline{\log \mathbf{c}} - \log(\overline{\mathbf{A}\mathbf{z}})) - \mathbf{h}(\mathbf{A}). \quad (20)$$